Cell cycle-targeting microRNAs promote differentiation by enforcing cell-cycle exit

Tobias Otto[a,b,1], Sheyla V. Candido[a], Mary S. Pilarz[a], Ewa Sicinska[c], Roderick T. Bronson[d], Michaela Bowden[e], Iga A. Lachowicz[a], Kristin Mulry[a], Anne Fassl[a,b], Richard C. Han[a], Emmanuelle S. Jecrois[a], and Piotr Sicinski[a,b,2]

[a]Department of Cancer Biology, Dana-Farber Cancer Institute, Boston, MA 02215; [b]Department of Genetics, Harvard Medical School, Boston, MA 02115; [c]Department of Oncologic Pathology, Dana-Farber Cancer Institute, Boston, MA 02215; [d]Rodent Histopathology Core, Dana-Farber/Harvard Cancer Center, Harvard Medical School, Boston, MA 02115; and [e]Department of Medical Oncology, Dana-Farber Cancer Institute, Boston, MA 02215

Edited by Terry L. Orr-Weaver, Whitehead Institute, Cambridge, MA, and approved August 24, 2017 (received for review February 22, 2017)

MicroRNAs (miRNAs) have been known to affect various biological processes by repressing expression of specific genes. Here we describe an essential function of the miR-34/449 family during differentiation of epithelial cells. We found that miR-34/449 suppresses the cell-cycle machinery in vivo and promotes cell-cycle exit, thereby allowing epithelial cell differentiation. Constitutive ablation of all six members of this miRNA family causes derepression of multiple cell cycle-promoting proteins, thereby preventing epithelial cells from exiting the cell cycle and entering a quiescent state. As a result, formation of motile multicilia is strongly inhibited in several tissues such as the respiratory epithelium and the fallopian tube. Consequently, mice lacking miR-34/449 display infertility as well as severe chronic airway disease leading to postnatal death. These results demonstrate that miRNA-mediated repression of the cell cycle is required to allow epithelial cell differentiation.

miR-34 | cell cycle | cyclins | epithelial differentiation | ciliogenesis

MicroRNAs (miRNAs) are ∼22-nt-long RNAs that participate in numerous cellular functions by posttranscriptionally regulating gene expression. Each miRNA is capable of repressing hundreds of mRNAs through pairing to sites in the 3′ untranslated regions of target transcripts (1). Each individual target is typically repressed only modestly (2), and regulation of cellular processes frequently depends on coregulation of several genes within one particular pathway. Understanding the physiological functions of miRNAs is frequently hampered by the extensive redundancy of miRNA regulatory networks.

Several miRNAs have been described as negative regulators of cell proliferation and potential suppressors of tumorigenesis. However, the biological relevance of such an miRNA-mediated regulation of the cell-cycle machinery in vivo remains unclear. One of the best-described examples of miRNAs that target cell-cycle proteins is the miR-34 family, which includes family members miR-34a, miR-34b, and miR-34c. These miRNAs have been described as targeting multiple components of the cell-cycle machinery including cyclin D1, cyclin E2, CDK4, CDK6, CDC25A, and E2F3 (3–7), and trigger cell-cycle arrest (mainly during G1 phase) and apoptosis (4, 8–11). Furthermore, miR-34 family members are frequently down-regulated in many human cancers, suggesting a potential role of this miRNA family as tumor suppressors (12).

Although originally designated as a separate miRNA family, miR-449a, miR-449b, and miR-449c possess identical seed sequences (i.e., nucleotides 2 to 7) as members of the miR-34 family. Indeed, all these miRNAs were shown to regulate an overlapping set of targets, and can hence be considered as one miRNA family, named miR-34/449 (13). miR-449a also induces cell-cycle arrest and apoptosis in vitro, and its expression is down-regulated in prostate cancer (14).

Most attempts to understand the function of miR-34/449 family members have relied on overexpression in cultured cells. In contrast, ablation of individual members of the miR-34/449 family in mice did not uncover any essential functions in vivo (15–17), apart from minor defects in bone development (18) and improved heart function during aging (19). Combined ablation of the miR-34/449 family revealed an essential role of these miRNAs during ciliogenesis in vivo (20, 21). This function was ascribed either to the ability of the miR-34/449 family to regulate the centrosomal protein CP110, thereby affecting docking of basal bodies to the cell membrane (20), or to regulation of Notch1 signaling (22). Independent of these studies, we generated mice with combined deletion of all three genomic loci of the miR-34/449 family to investigate the physiological role of these miRNAs in vivo. Our analyses uncovered an essential function of the miR-34/449 family in controlling the balance between cell proliferation and differentiation.

Results

Ablation of All miR-34/449 Members Causes Postnatal Lethality in Mice. We started our analyses by comparing the expression levels of all major transcripts of the miR-34/449 family in tissues from wild-type adult mice (Fig. S1*A*). We found that miR-34a was expressed ubiquitously, whereas miR-34b/c and miR-449a/b/c expression was restricted mainly to lungs, female reproductive organs (ovaries and fallopian tubes), and testes.

We then generated knockout strains of mice lacking miR-34a, miR-34b/c, or miR-449a/b/c (Fig. S1 *B–D*). None of these single-miRNA locus knockout (KO) as well as miR-34 "double-knockout" (DKO) mice displayed any apparent abnormalities.

Significance

The interplay between microRNAs and the cell-cycle machinery in vivo remains poorly understood. Here we report that the microRNA family miR-34/449 plays an essential and rate-limiting role in repressing cell-cycle proteins and enforcing cell-cycle exit during epithelial cell differentiation. We demonstrate that genetic ablation of the entire miR-34/449 family leads to derepression of cell cycle-promoting proteins in differentiating epithelial cells, thereby preventing their timely cell-cycle exit. This, in turn, impairs epithelial ciliation and leads to profound developmental defects. Hence, this study describes a function of the miR-34/449 family in linking cell proliferation and differentiation.

Author contributions: T.O. and P.S. designed research; T.O., S.V.C., M.S.P., E.S., M.B., I.A.L., K.M., A.F., R.C.H., and E.S.J. performed research; T.O., E.S., R.T.B., M.B., and P.S. analyzed data; and T.O. and P.S. wrote the paper.

Conflict of interest statement: P.S. declares that he is a consultant for and receives research funding from Novartis.

This article is a PNAS Direct Submission.

Data deposition: The cDNA microarray data reported in this paper have been deposited in the Gene Expression Omnibus (GEO) database, https://www.ncbi.nlm.nih.gov/geo (accession no. GSE92296).

[1]Present address: Department of Internal Medicine III, University Hospital Rheinisch-Westfälische Technische Hochschule (RWTH) Aachen, Aachen 52074, Germany.

[2]To whom correspondence should be addressed. Email: peter_sicinski@dfci.harvard.edu.

This article contains supporting information online at www.pnas.org/lookup/suppl/doi:10.1073/pnas.1702914114/-/DCSupplemental.

Subsequently, we obtained "triple-knockout" (TKO) mice by interbreeding mice lacking miR-34a, miR-34b/c, and miR-449a/b/c loci. Although TKO mice were born at the expected frequency [expected, 25%; observed, 78 out of 284 (27%) newborn mice], almost 80% of mice died within the first 4 wk (Fig. 1*A*). Knockout neonates failed to thrive and exhibited reduced body weights (Fig. 1*B*), severe inflammation (with accumulation of neutrophil granulocytes and debris) in the nasal cavity (Fig. 1*C*), as well as opportunistic bacterial infection with gram-negative *Pasteurella pneumotropica* (*SI Materials and Methods*).

To confirm that the bacterial infection was responsible for the observed lethality, we treated pregnant females and newborn mice with enrofloxacin, a broad-spectrum antibiotic. Indeed, this treatment led to an almost complete rescue of postnatal lethality (Fig. 1*D*), as well as a rescue of the weight loss in neonatal TKO mice (Fig. 1*E*). Moreover, enrofloxacin-treated TKO mice that survived the first 5 wk showed essentially normal life spans (Fig. S1*E*). Despite reports that miR-34/449 family members have tumor-suppressive properties (12), we observed no increase in tumor incidence in TKO animals (Fig. S1*F*).

TKO Mice Show Defective Multiciliogenesis in Several Tissues. We next investigated the cause of the infections in TKO mice. An important mechanism that prevents infections by pathogens in the airways is the coordinated beating of motile multicilia that cover the respiratory epithelium. Therefore, we analyzed the respiratory epithelium for the presence of multicilia. As expected, the respiratory epithelium of wild-type and miR-34 DKO mice exhibited an almost complete coverage with multicilia (Fig. 2*A*). In contrast, the extent of ciliation in the nasal respiratory epithelium of TKO mice was severely reduced (Fig. 2*A*). Similarly, we observed an absence of normal ciliation in the respiratory epithelium of the trachea, bronchi, and bronchioles (Fig. 2*B*). Importantly, the

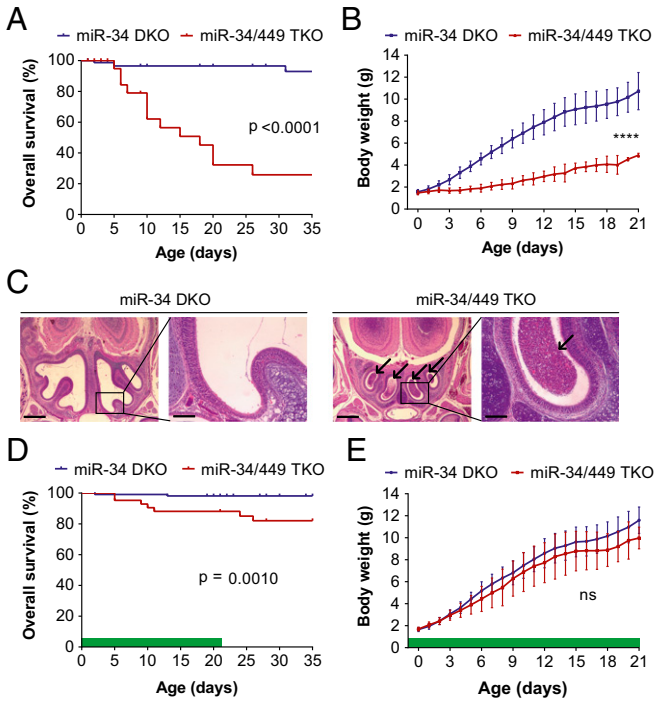

Fig. 1. miR-34/449 TKO mice display postnatal lethality resulting from chronic airway disease. (*A*) Survival of mice lacking all miR-34/449 members (miR-34/449 TKO; $n = 17$) compared with littermates lacking miR-34a/b/c (miR-34 DKO; $n = 28$). Log-rank test. (*B*) Body weight of miR-34 TKO mice ($n = 11$) compared with miR-34 DKO littermates ($n = 26$). Data are presented as mean ± SD; $^{****}P < 0.0001$ (for days 4 to 21); two-way ANOVA with Bonferroni's multiple comparisons test (for each day). (*C*) Histological sections of the nasal cavities from 2-d-old miR-34 DKO and miR-34/449 TKO littermates, stained with hematoxylin and eosin (HE). Arrows indicate accumulation of debris and neutrophils. [Scale bars, 500 μm (*Left* for each group) and 100 μm (*Right* for each group).] (*D*) Survival of miR-34/449 TKO mice ($n = 42$) compared with miR-34 DKO littermates ($n = 107$). Both groups were treated with the antibiotic enrofloxacin until weaning (day 21), as indicated by a green line. Log-rank test. (*E*) Body weight of miR-34 TKO mice ($n = 9$) compared with miR-34 DKO littermates ($n = 17$), treated as in *D*. Data are presented as mean ± SD; ns, not significant; two-way ANOVA with Bonferroni's multiple comparisons test.

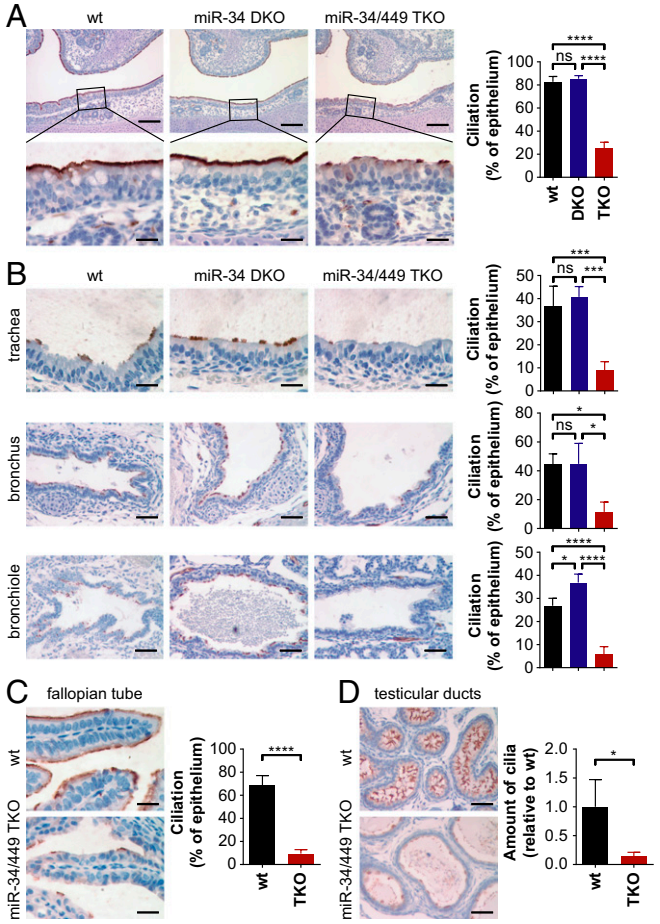

Fig. 2. Impaired multiciliogenesis in multiple tissues of miR-34/449 TKO mice. (*A*) Histological sections of the nasal respiratory epithelium from wild-type (wt), miR-34 DKO, and miR-34/449 TKO embryos at E18.5, stained for the cilia marker K40-acetylated α-tubulin (brown). [Scale bars, 100 μm (*Upper*) and 20 μm (*Lower*).] (*A*, *Right*) Quantification of ciliation as the percentage of epithelium covered with cilia using K40-acetylated α-tubulin–stained sections from wt ($n = 3$), miR-34 DKO ($n = 3$), and miR-34/449 TKO ($n = 3$) embryos. Data are presented as mean ± SD; $^{****}P < 0.0001$; ns, not significant; one-way ANOVA with Tukey's multiple comparisons test. (*B*) Histological sections of the trachea (*Upper*), bronchus (*Middle*), and bronchiole (*Lower*) from wild-type, miR-34 DKO, and miR-34/449 TKO embryos at E18.5, stained as in *A*. [Scale bars, 20 μm (*Upper* and *Lower*) and 50 μm (*Middle*).] (*B*, *Right*) Quantification as in *A*. Data are presented as mean ± SD; $^{****}P < 0.0001$, $^{***}P < 0.001$, $^{*}P < 0.05$; ns, not significant. (*C*) Histological sections of the fallopian tube epithelium from 6-wk-old wt and miR-34/449 TKO mice, stained as in *A*. (Scale bars, 20 μm.) (*C*, *Right*) Quantification as in *A* using histological sections from wt ($n = 10$) and miR-34/449 TKO ($n = 5$) mice. Data are presented as mean ± SD; $^{****}P < 0.0001$; unpaired *t* test. (*D*) Histological sections of testicular efferent ducts from 6-wk-old w-t and miR-34/449 TKO mice, stained as in *A*. (Scale bars, 50 μm.) (*D*, *Right*) Quantification of ciliation as the total amount of brown staining per image using K40-acetylated α-tubulin–stained sections from wt ($n = 6$) and miR-34/449 TKO ($n = 4$) mice. Data are presented as mean ± SD, relative to the mean amount of cilia staining in the wt group; $^{*}P < 0.05$; unpaired *t* test with Welch's correction.

typical "9 + 2" microtubular structure of these motile cilia was unaltered in TKO embryos (Fig. S2*A*). The lack of multicilia in the respiratory epithelium most likely explains the postnatal lethality of TKO mice, since continuous beating of cilia is required for proper elimination of debris and bacteria.

In addition to the respiratory epithelium, motile cilia cover the epithelial surface of several other compartments. We found that the fallopian tube epithelium of TKO females displayed a severe reduction of multicilia (Fig. 2*C*). We also observed a strong reduction in the amount of multicilia in the efferent ducts of the testes (Fig. 2*D*). In contrast, other ciliated tissues (including the multiciliated ependymal cells lining the brain ventricles and the monociliated cells of the olfactory epithelium and kidney) did not display any apparent ciliation defects (Fig. S2 *B–E*), consistent with the tissue-restricted expression pattern of most miR-34/449 family members (Fig. S1*A*).

Ablation of miR-34/449 Members Leads to Infertility in Female and Male Mice. The observation of ciliogenesis defects in the reproductive organs prompted us to investigate the fertility of TKO mice. When mated with wild-type males, female TKO mice were unable to produce offspring. Importantly, TKO females showed unperturbed ovarian histology, with the presence of corpora lutea indicating normal ovulation (Fig. S2*F*). To further investigate the reason for infertility, we superovulated animals and analyzed the fate of ovulated oocytes by histology. As expected, by 2.5 d postsuperovulation, oocytes in control mice reached the ampulla of the fallopian tube, a site where fertilization takes place (Fig. 3 *A* and *B*). In contrast, in TKO females, the ovulated oocytes were trapped in the bursa of the ovary (Fig. 3 *A* and *B*). Since oocyte migration critically depends on cilia function, the loss of multicilia in the fallopian tube is most likely responsible for the infertility of female TKO mice.

Cilia are also essential for maintaining male fertility. We found that seven out of eight TKO males were incapable of impregnating wild-type females. Histological analysis of testes demonstrated atrophy of the testicular tubules starting at the age of 5 wk (Fig. 3*C*). Furthermore, analyses of sperm content within the cauda epididymis revealed a strong reduction of sperm counts in TKO males (Fig. 3*D*). These observations suggest that the ciliogenesis defect in the efferent ducts of the testes compromises the movement of sperm from the testis into the epididymis, and likely contributes to infertility in TKO males.

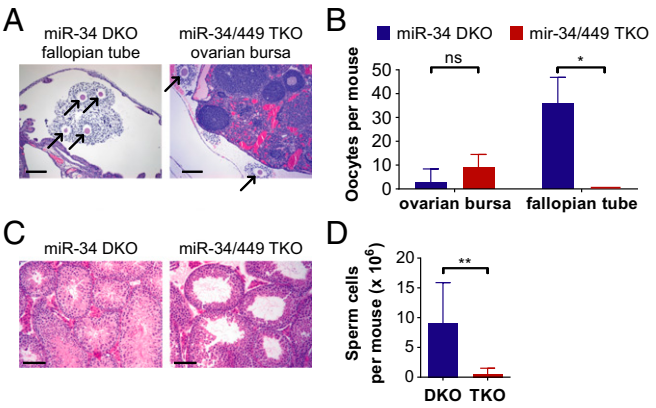

Fig. 3. miR-34/449 TKO mice exhibit defects in female and male reproductive organs. (*A*) Histological sections showing oocytes in the fallopian tube (ampulla) of an miR-34 DKO mouse and in the ovarian bursa of an miR-34/449 TKO mouse, 16 h after injection with human chorionic gonadotropin (hCG). Sections were stained with HE. (Scale bars, 200 μm.) Arrows point to oocytes. (*B*) Number of oocytes detected in histological sections of ovaries and fallopian tubes from 4-wk-old miR-34/449 TKO ($n = 4$) and miR-34 DKO mice ($n = 5$), 16 h after injection with hCG. Data are presented as mean ± SD; $^*P < 0.05$; ns, not significant; Mann–Whitney test. (*C*) Histological sections of testes from 5-wk-old miR-34 DKO and miR-34/449 TKO littermates, stained with HE. (Scale bars, 100 μm.) (*D*) Number of sperm cells isolated from the cauda epididymis of 8-wk-old miR-34 DKO ($n = 12$) and miR-34/449 TKO ($n = 9$) mice. Data are presented as mean ± SD; $^{**}P < 0.01$; Mann–Whitney test.

TKO Animals Display Normal Cell-Fate Specification. We next investigated the cellular basis of the ciliogenesis defects in TKO animals. Multicilia formation in the respiratory epithelium requires cell-fate specification into progenitors of multiciliated columnar epithelial cells, which are characterized by expression of the transcription factor FOXJ1. Staining with an anti-FOXJ1 antibody revealed an unperturbed proportion of FOXJ1-positive progenitor cells in TKO respiratory epithelium (Fig. S2*G*). Likewise, we observed only minor changes in the proportion of mucus-producing goblet cells and undifferentiated basal cells (Fig. S2 *H* and *I*). We concluded that the mutant epithelium undergoes normal cell-fate specification and hence the observed defects cannot be explained by the absence of cilia-producing cells.

miR-34/449 Ablation Causes Up-Regulation of Cell-Cycle Genes in the Respiratory Epithelium. To understand the molecular basis of the defect in ciliogenesis in TKO mice, we analyzed gene expression changes in the respiratory epithelium upon miR-34/449 ablation. For analysis, we chose embryos at embryonic day 16.5 (E16.5), that is, shortly after the onset of ciliogenesis, to detect primary expression changes in the mutant epithelium. We isolated nasal respiratory epithelium from wild-type and TKO embryos using laser capture microdissection and compared global gene expression using cDNA microarrays. We detected significant expression changes of 480 mRNAs (Fig. 4*A*). As expected from the repressive function of miRNAs, most of these deregulated mRNAs (398 out of 480; i.e., 83%) displayed up-regulated levels upon miRNA ablation. Notably, mRNAs up-regulated in TKO epithelium were enriched for transcripts containing predicted target sites of the miR-34/449 major strand (5p) seed sequence in their 3′ UTR, indicating their direct regulation by miR-34/449 (Fig. S3 *A* and *B*).

We next analyzed these deregulated mRNAs for enrichment of biological processes. Strikingly, the cell cycle represented the only biological process/pathway significantly enriched among deregulated mRNAs (Table S1). Indeed, 40 out of 457 deregulated mRNAs were functionally associated with the cell cycle, and most of these cell-cycle genes (37 out of 40) were up-regulated in the respiratory epithelium upon miR-34/449 ablation (Fig. 4*B*). We confirmed gene expression changes for 10 of these cell-cycle genes using RT-qPCR (Fig. 4*C*). In contrast, genes functionally associated with "lung/multiciliated epithelial cell differentiation" or "ciliogenesis regulation" were overall not deregulated, including no significant changes in mRNA levels of *Ccp110*, a gene implicated in negative regulation of ciliogenesis (20) (Fig. S3 *C* and *D*). Since Notch1 pathway activation is well-known to affect cell-fate specification (23), we searched our mRNA expression data for an indication of Notch1 activation. However, among 188 genes described as Notch1 target genes (24), only 5 were significantly deregulated in the respiratory epithelium of TKO embryos, indicating that Notch1 signaling is not activated upon miR-34/449 ablation (Fig. S3*E*).

miR-34/449 Ablation Increases the Levels of Cell-Cycle Proteins and Enhances Proliferation in Multiciliated Epithelia. Given the well-established notion that cells must exit the cell cycle to start ciliogenesis, we hypothesized that increased levels of cell-cycle proteins might retain differentiating cells in a proliferative state and prevent cell-cycle exit, thereby blocking normal ciliogenesis. To test this, we analyzed protein levels of some of the up-regulated cell-cycle genes in the upper cell layer of the respiratory epithelium, which almost exclusively consists of multiciliated columnar epithelial cells. Consistent with changes in mRNA levels, we

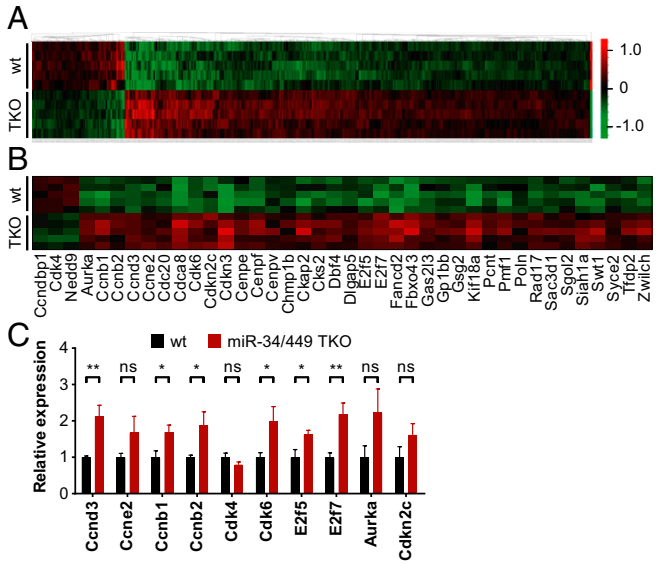

Fig. 4. Ablation of miR-34/449 causes up-regulation of cell-cycle genes in the respiratory epithelium. (*A*) A heat map showing gene expression changes in the nasal respiratory epithelium from miR-34/449 TKO ($n = 5$) compared with wild-type ($n = 5$) embryos at E16.5. Expression of 480 significantly deregulated genes (columns) across the analyzed embryos (rows) identified by cDNA microarray, using a cutoff for significance (false discovery rate < 0.05) and expression (fold change > 1.2), sorted according to supervised hierarchical clustering, with expression changes indicated as log2 values relative to the mean expression for each gene (red, up-regulated; green, down-regulated). (*B*) A heat map showing gene expression changes in the nasal respiratory epithelium from miR-34/449 TKO ($n = 5$) compared with wild-type ($n = 5$) embryos at E16.5, presented as in *A*, showing only 40 genes enriched in the Gene Ontology process "cell cycle." Expression changes are indicated as in *A*. (*C*) RT-qPCR validation of gene expression changes for selected cell-cycle genes in the nasal respiratory epithelium from miR-34/449 TKO ($n = 4$) compared with wild-type ($n = 4$) embryos at E16.5. Data are presented as mean expression ± SD, normalized to Actb and Gapdh transcript levels, relative to the mean of the wt group; $^{**}P < 0.01$, $^{*}P < 0.05$; ns, not significant; unpaired *t* tests with multiple comparison correction using the Holm–Sidak method.

observed a strong increase of cyclin D3 and cyclin B1 protein levels in the respiratory epithelium of TKO embryos (Fig. 5*A*), as well as an up-regulation of cyclin B1, cyclin A2, CDC25A, *N*-MYC, Aurora A, and CDK1 in the fallopian tube of TKO females (Fig. 5*B*). In contrast, we observed no increase of CP110 (encoded by *Ccp110*) in the fallopian tube (Fig. 5*B*) or trachea of TKO mice (Fig. S4*A*). Collectively, these results established a widespread up-regulation of cell cycle-regulating proteins in multiciliated epithelia of TKO mice.

We next asked whether the increased levels of cell-cycle proteins led to unscheduled proliferation of epithelial cells in TKO mice. Indeed, the fraction of proliferating cells was significantly elevated in the respiratory and fallopian tube epithelium of TKO mice, as revealed by Ki67 staining, proliferating cell nuclear antigen (PCNA) staining, as well as BrdU incorporation (Fig. 5 *C*–*F*). Moreover, the percentage of proliferating cells inversely correlated with the extent of ciliation (Fig. S4*B*). In contrast, ablation of miR-34/449 members did not affect the proliferation in the intestinal epithelium (Fig. S4*C*). Taken together, these analyses revealed that mice lacking the miR-34/449 family display elevated levels of several cell cycle-regulating proteins in specific epithelial compartments, thereby retaining epithelial cells in a proliferative state and preventing their exit from the cell cycle.

Increased Activity of Cyclin-Dependent Kinases Is Responsible for the Multiciliogenesis Defect in TKO Mice. We hypothesized that the inability of TKO respiratory epithelial cells to normally exit the cell cycle, due to an up-regulation of cell-cycle proteins, represented the direct cause of the ciliogenesis defect. To test this, we asked whether inhibition of the hyperactivated cell-cycle machinery might correct the phenotypic abnormalities seen in TKO animals. We treated newborn TKO mice with a panel of inhibitors of cyclin-dependent kinases (CDKs): ribociclib (which inhibits CDK4 and CDK6), roscovitine (which inhibits CDK1, CDK2, and CDK7), and R547 (which inhibits CDK1, CDK2, and CDK5). In the case of ribociclib, we confirmed that administration of this inhibitor to TKO animals extinguished aberrant cell proliferation in the respiratory epithelium (Fig. 6*A* and Fig. S5*A*). Prolonged

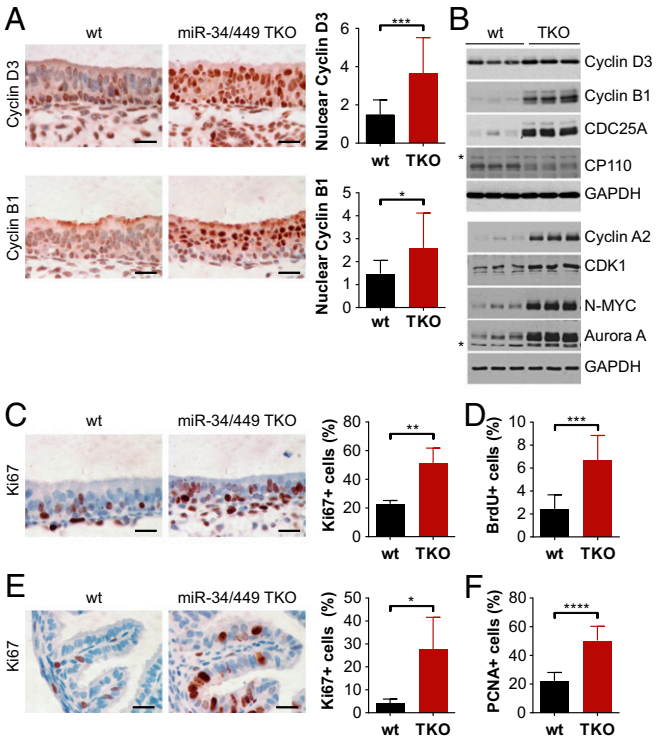

Fig. 5. Ablation of miR-34/449 activates the cell-cycle machinery, resulting in abnormal proliferation. (*A*) Histological sections of the nasal respiratory epithelium from wild-type and miR-34/449 TKO embryos at E16.5, stained for cyclin D3 (*Upper*, brown) and cyclin B1 (*Lower*, brown). (Scale bars, 20 μm.) (*A*, *Right*) Quantification of average staining intensity per nucleus among columnar epithelial cells using histological sections from wt ($n = 10$) and miR-34/449 TKO ($n = 10$) embryos. Data are presented as mean ± SD; $^{***}P < 0.001$, $^{*}P < 0.05$; Mann–Whitney test (*Upper*), unpaired *t* test with Welch's correction (*Lower*). (*B*) Western blot analysis of fallopian tubes from 6-wk-old wild-type and miR-34/449 TKO mice, probed with antibodies against the indicated proteins. GAPDH served as a loading control. Asterisks indicate nonspecific bands. (*C*) Histological sections of the nasal respiratory epithelium as in *A*, stained for the proliferation marker Ki67 (brown). (Scale bars, 20 μm.) (*C*, *Right*) Quantification of the percentage of columnar epithelial cells that exhibited nuclear Ki67 staining (Ki67^{+}) using histological sections from wild-type ($n = 3$) and miR-34/449 TKO ($n = 8$) embryos. Data are presented as mean ± SD; $^{**}P < 0.01$; unpaired *t* test. (*D*) Quantification of the percentage of columnar epithelial cells with nuclear BrdU staining (BrdU^{+}) using sections from wild-type ($n = 8$) and miR-34/449 TKO ($n = 7$) embryos (E16.5). Data are presented as mean ± SD; $^{***}P < 0.001$; unpaired *t* test. (*E*) Histological sections of fallopian tubes from 6-wk-old wild-type and miR-34/449 TKO mice, stained for Ki67 (brown). (Scale bars, 20 μm.) (*E*, *Right*) Quantification of the percentage of fallopian tube epithelial cells with nuclear Ki67 staining (Ki67^{+}) using sections from wt ($n = 10$) and miR-34/449 TKO ($n = 5$) mice. Data are presented as mean ± SD; $^{*}P < 0.05$; unpaired *t* test with Welch's correction. (*F*) Quantification of the percentage of fallopian tube epithelial cells with nuclear PCNA staining (PCNA^{+}) using sections from 6-wk-old wild-type ($n = 9$) and miR-34/449 TKO ($n = 4$) mice. Data are presented as mean ± SD; $^{****}P < 0.0001$; unpaired *t* test.

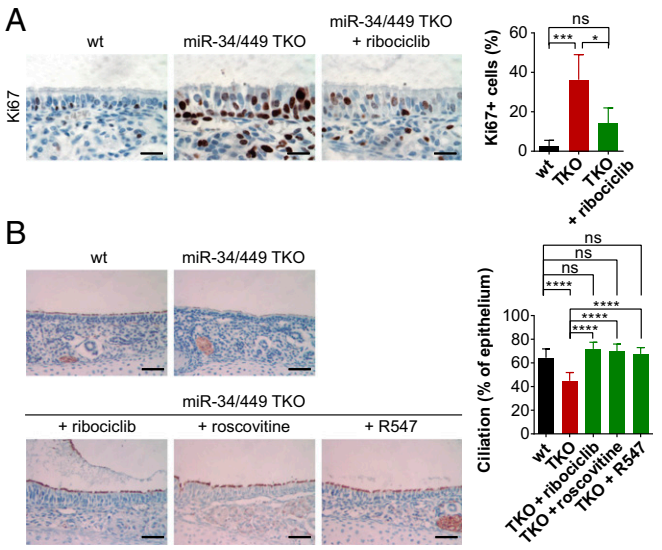

Fig. 6. CDK inhibition rescues the ciliogenesis defect in miR-34/449 TKO mice. (*A*) Histological sections of the nasal respiratory epithelium from wild-type and miR-34/449 TKO mice treated for 48 h with PBS, and miR-34/449 TKO mice treated for 48 h with ribociclib, stained for the proliferation marker Ki67 (brown). (Scale bars, 20 μm.) (*A*, *Right*) Quantification of the percentage of columnar epithelial cells with nuclear Ki67 staining (Ki67$^+$) using sections from at least three mice per group. Data are presented as mean ± SD; $***P < 0.001$, $*P < 0.05$; ns, not significant; one-way ANOVA with Tukey's multiple comparisons test. (*B*) Histological sections of the nasal respiratory epithelium from wild-type and miR-34/449 TKO mice treated for 7 d with PBS, as well as miR-34/449 TKO mice treated for 7 d with the CDK inhibitors ribociclib, roscovitine, or R547. Sections were stained for the cilia marker K40-acetylated α-tubulin (brown). (Scale bars, 50 μm.) (*B*, *Right*) Quantification of ciliation as the percentage of epithelium covered with cilia using sections from at least eight mice per group. Data are presented as mean ± SD; $****P < 0.0001$; ns, not significant; one-way ANOVA with Tukey's multiple comparisons test.

treatment with each of these inhibitors fully corrected the phenotypic abnormalities seen in TKO animals (Fig. 6*B*). We found that the extent of ciliation in the respiratory epithelium of inhibitor-treated TKO mice was identical to that of untreated wild-type mice (Fig. 6*B*). We concluded that an increased CDK activity resulting from increased levels of cyclins and CDKs represented the direct cause of the ciliogenesis defect in TKO mice. Collectively, our results reveal that members of the miR-34/449 family play an essential and rate-limiting role during epithelial differentiation, by repressing the cell-cycle machinery and promoting cell-cycle exit (Fig. S5*C*).

Discussion

Since their discovery, miRNAs have been implicated in a wide range of biological processes. Early studies revealed that expression of miRNAs is relatively tissue-specific, correlates with the differentiation state, and is generally down-regulated in human cancers (25). These observations suggested that miRNAs may function to restrain cell proliferation, to prevent tumorigenesis, and to promote differentiation. Members of the miR-34/449 family represent one of the best-studied examples of miRNAs with potentially antiproliferative roles. These miRNAs possess various growth-suppressive functions such as induction of apoptosis and cell-cycle arrest in vitro (4, 8–11, 26, 27). Consistent with a growth-suppressive role for miR-34a, its genetic ablation was shown to enhance tumorigenesis in mouse models of KRAS^{G12D};p53$^{+/-}$ lung cancer (28), p53$^{-/-}$ prostate cancer (29), carcinogen-induced colon cancer (30), and *SmoA1*-overexpressing medulloblastoma (31). In contrast, we observed that mice lacking all members of the miR-34/449 family did not display any increase in spontaneous tumorigenesis. These results suggest that while miR-34a suppresses tumorigenesis in the context of certain oncogenic lesions, deletion of all miR-34/449 members is insufficient to cause cancer formation.

We report here that deletion of all members of the miR-34/449 family results in derepression of cell-cycle proteins and triggers unscheduled proliferation in several differentiating tissues. Furthermore, we demonstrate that failure of cells to timely exit the cell cycle is responsible for impaired epithelial cell differentiation, namely it blocks formation of motile multicilia. It is well-established that ciliogenesis requires cells to exit the cell cycle. Once rendered quiescent, cells then assemble cilia in an ordered process. This can be reversed by ciliary resorption, which occurs upon cell-cycle reentry and allows the centrioles to be used as spindle poles during mitosis (32). Therefore, the lack of cilia in proliferating cells likely represents a combined result of suppression of cilia formation as well as enhanced ciliary resorption.

The defect in ciliogenesis observed upon genetic deletion of all miR-34/449 family genes in mice resembles some symptoms of human primary ciliary dyskinesia (PCD), such as chronic airway disease and reduced fertility in females and males. However, unlike TKO mice, PCD patients suffer from reduced cilia motility, commonly caused by mutations that trigger ultrastructural defects of the ciliary axoneme. Moreover, abnormalities such as situs inversus and hydrocephalus, which also occur in a subset of PCD patients, were not observed in TKO mice. It should be noted that expression of the miR-34b/c and miR-449a/b/c genes is restricted to only a few tissues, including respiratory epithelium, fallopian tubes, and testes, and their expression increases during multiciliogenesis in vitro (33). The tissue-specific expression of these miRNAs likely explains why ciliogenesis in other tissues is not affected. We speculate that in these tissues, other microRNAs are responsible for repression of the cell-cycle machinery during differentiation and ciliogenesis.

Two earlier studies implicated the miR-34/449 family in regulation of ciliogenesis in vivo. The first study reported that miR-449 regulates ciliogenesis by repressing Notch1 signaling (22). However, we did not observe any evidence of activation of Notch1 signaling in the respiratory epithelium of TKO mice (Fig. S3*E*). Moreover, Notch1 activation is well-known to affect cell-fate specification by favoring the formation of mucus-producing goblet cells at the expense of cilia-generating columnar epithelial cells (23), a phenotype not seen in TKO mice (Fig. S2 *G* and *H*). The second report implicated CP110 as a regulator of ciliogenesis operating downstream of miR-34/449 (20). The authors proposed that increased levels of CP110 prevent docking of the basal bodies to the cell membrane. However, we found that ablation of miR-34/449 had no effect on the levels of CP110 transcripts and protein in the nasal respiratory epithelium at the time of multicilia formation (Fig. S3 *C* and *D*), in the trachea (Fig. S4*A*), or in the fallopian tube epithelium (Fig. 5*B*). Therefore, we conclude that, while alterations of Notch1 signaling and CP110 may contribute to the observed phenotype, it is unlikely that they represent the major primary molecular lesion responsible for the differentiation defects seen in TKO mice.

In contrast to these findings, we observed that ablation of miR-34/449 triggered an enhanced expression of almost 40 cell cycle-promoting genes. Of note, the cell cycle was the only biological process significantly enriched among genes deregulated in the respiratory epithelium of TKO mice at the time when ciliogenesis takes place in vivo. These cell cycle-promoting proteins are well-known to drive cell-cycle progression by increasing the activity of cyclin-dependent kinases. Indeed, we observed that ablation of miR-34/449 increased proliferation of epithelial cells and prevented cell-cycle exit. Importantly, inhibition of abnormal CDK activity corrected the phenotype seen in TKO mice and restored normal ciliogenesis in miR-34/449–deficient animals. These results indicate that expression of miR-34/449 is essential for these cells to exit the cell cycle and enter quiescence, or to maintain cells in a quiescent state. Several cell-cycle genes were previously shown to

represent direct targets of miR-34/449 family members, including cyclin D3 (34), cyclin B1 (22), CDC25A (7), and *N*-MYC (35). Hence, increased expression of these cell-cycle proteins in TKO mice represents a direct effect of their derepression upon miR-34/449 ablation.

miRNAs of the miR-34/449 family were also reported to be involved in spermatogenesis (21, 36, 37). In particular, miR-34b/c and miR-449a/b/c are required for proper execution of meiosis in male gametes and during the maturation of spermatids (36). It is likely that both the involvement of this miRNA family in spermatogenesis as well as their role in multicilia formation in the efferent ducts of the testes, described in our study, contribute to the infertility observed in male TKO mice. Further experiments using tissue-specific deletion of these miRNAs will allow dissecting the relative contribution of these defects to male infertility.

In summary, our study establishes the miR-34/449 family as an essential and rate-limiting regulator of epithelial differentiation in vivo, acting via suppression of cell-cycle genes. Ablation of miR-34/449 derepresses the cell-cycle machinery, thereby preventing epithelial cell differentiation. In addition to uncovering a novel function for cell cycle-targeting miRNAs during normal development, these findings may have implications for the mechanisms responsible for human ciliopathies as well as for novel therapeutic strategies for patients with cilia defects.

Materials and Methods

Treatment of miR-34/449 TKO Mice. For inhibition of CDKs, newborn mice were treated by daily i.p. injection with the CDK inhibitors ribociclib (200 mg/kg body weight), roscovitine (5 mg/kg), R547 (2 mg/kg), or, for control, PBS (25 mL/kg). All animal experiments were approved by the Institutional Animal Care and Use Committee of the Dana-Farber Cancer Institute and were carried out in accordance with approved protocols and regulatory standards. Details are provided in *SI Materials and Methods* and Table S2.

Laser Capture Microdissection and Microarray Analysis. The respiratory epithelium cell layer was isolated from formalin-fixed paraffin-embedded sections of embryonic heads using laser capture microdissection. Subsequently, RNA was extracted and cDNA microarray analysis was performed using the SensationPlus FFPE Amplification and WT Labeling Kit and Mouse Gene v2.0 ST array chips (Affymetrix). Details are provided in *SI Materials and Methods*.

Histology, RT-qPCR, and Western Blot Analysis. These procedures were performed according to established protocols. Details are provided in *SI Materials and Methods* and Table S2.

ACKNOWLEDGMENTS. We thank Drs. Sanny S. Chung and Debra J. Wolgemuth for advice, and Carolina Vazquez, Justyna Rozycka, Anran Li, Xiaoting Li, and Jeffrey T. Czaplinski for help. This work was supported by National Cancer Institute, National Institutes of Health, Department of Health and Human Services Grants R01 CA083688 and CA132740 (to P.S.).

1. Bartel DP (2009) MicroRNAs: Target recognition and regulatory functions. *Cell* 136:215–233.
2. Baek D, et al. (2008) The impact of microRNAs on protein output. *Nature* 455:64–71.
3. Welch C, Chen Y, Stallings RL (2007) MicroRNA-34a functions as a potential tumor suppressor by inducing apoptosis in neuroblastoma cells. *Oncogene* 26:5017–5022.
4. He L, et al. (2007) A microRNA component of the p53 tumour suppressor network. *Nature* 447:1130–1134.
5. Sun F, et al. (2008) Downregulation of CCND1 and CDK6 by miR-34a induces cell cycle arrest. *FEBS Lett* 582:1564–1568.
6. Lujambio A, et al. (2008) A microRNA DNA methylation signature for human cancer metastasis. *Proc Natl Acad Sci USA* 105:13556–13561.
7. Yang X, et al. (2009) miR-449a and miR-449b are direct transcriptional targets of E2F1 and negatively regulate pRb-E2F1 activity through a feedback loop by targeting CDK6 and CDC25A. *Genes Dev* 23:2388–2393.
8. Raver-Shapira N, et al. (2007) Transcriptional activation of miR-34a contributes to p53-mediated apoptosis. *Mol Cell* 26:731–743.
9. Chang TC, et al. (2007) Transactivation of miR-34a by p53 broadly influences gene expression and promotes apoptosis. *Mol Cell* 26:745–752.
10. Tarasov V, et al. (2007) Differential regulation of microRNAs by p53 revealed by massively parallel sequencing: miR-34a is a p53 target that induces apoptosis and G1-arrest. *Cell Cycle* 6:1586–1593.
11. Bommer GT, et al. (2007) p53-mediated activation of miRNA34 candidate tumor-suppresser genes. *Curr Biol* 17:1298–1307.
12. Agostini M, Knight RA (2014) miR-34: From bench to bedside. *Oncotarget* 5:872–881.
13. Lizé M, Klimke A, Dobbelstein M (2011) MicroRNA-449 in cell fate determination. *Cell Cycle* 10:2874–2882.
14. Noonan EJ, et al. (2009) miR-449a targets HDAC-1 and induces growth arrest in prostate cancer. *Oncogene* 28:1714–1724.
15. Choi YJ, et al. (2011) miR-34 miRNAs provide a barrier for somatic cell reprogramming. *Nat Cell Biol* 13:1353–1360.
16. Bao J, et al. (2012) MicroRNA-449 and microRNA-34b/c function redundantly in murine testes by targeting E2F transcription factor-retinoblastoma protein (E2F-pRb) pathway. *J Biol Chem* 287:21686–21698.
17. Concepcion CP, et al. (2012) Intact p53-dependent responses in miR-34-deficient mice. *PLoS Genet* 8:e1002797.
18. Wei J, et al. (2012) miR-34s inhibit osteoblast proliferation and differentiation in the mouse by targeting SATB2. *J Cell Biol* 197:509–521.
19. Boon RA, et al. (2013) MicroRNA-34a regulates cardiac ageing and function. *Nature* 495:107–110.
20. Song R, et al. (2014) miR-34/449 miRNAs are required for motile ciliogenesis by repressing cp110. *Nature* 510:115–120.
21. Wu J, et al. (2014) Two miRNA clusters, miR-34b/c and miR-449, are essential for normal brain development, motile ciliogenesis, and spermatogenesis. *Proc Natl Acad Sci USA* 111:E2851–E2857.
22. Marcet B, et al. (2011) Control of vertebrate multiciliogenesis by miR-449 through direct repression of the Delta/Notch pathway. *Nat Cell Biol* 13:693–699.
23. Tsao PN, et al. (2009) Notch signaling controls the balance of ciliated and secretory cell fates in developing airways. *Development* 136:2297–2307.
24. Wang H, et al. (2011) Genome-wide analysis reveals conserved and divergent features of Notch1/RBPJ binding in human and murine T-lymphoblastic leukemia cells. *Proc Natl Acad Sci USA* 108:14908–14913.
25. Lu J, et al. (2005) MicroRNA expression profiles classify human cancers. *Nature* 435:834–838.
26. Corney DC, Flesken-Nikitin A, Godwin AK, Wang W, Nikitin AY (2007) MicroRNA-34b and microRNA-34c are targets of p53 and cooperate in control of cell proliferation and adhesion-independent growth. *Cancer Res* 67:8433–8438.
27. Tazawa H, Tsuchiya N, Izumiya M, Nakagama H (2007) Tumor-suppressive miR-34a induces senescence-like growth arrest through modulation of the E2F pathway in human colon cancer cells. *Proc Natl Acad Sci USA* 104:15472–15477.
28. Okada N, et al. (2014) A positive feedback between p53 and miR-34 miRNAs mediates tumor suppression. *Genes Dev* 28:438–450.
29. Cheng CY, et al. (2014) miR-34 cooperates with p53 in suppression of prostate cancer by joint regulation of stem cell compartment. *Cell Rep* 6:1000–1007.
30. Rokavec M, et al. (2014) IL-6R/STAT3/miR-34a feedback loop promotes EMT-mediated colorectal cancer invasion and metastasis. *J Clin Invest* 124:1853–1867.
31. Thor T, et al. (2015) miR-34a deficiency accelerates medulloblastoma formation in vivo. *Int J Cancer* 136:2293–2303.
32. Izawa I, Goto H, Kasahara K, Inagaki M (2015) Current topics of functional links between primary cilia and cell cycle. *Cilia* 4:12.
33. Lizé M, Herr C, Klimke A, Bals R, Dobbelstein M (2010) MicroRNA-449a levels increase by several orders of magnitude during mucociliary differentiation of airway epithelia. *Cell Cycle* 9:4579–4583.
34. Lal A, et al. (2011) Capture of microRNA-bound mRNAs identifies the tumor suppressor miR-34a as a regulator of growth factor signaling. *PLoS Genet* 7:e1002363.
35. Wei JS, et al. (2008) The MYCN oncogene is a direct target of miR-34a. *Oncogene* 27:5204–5213.
36. Comazzetto S, et al. (2014) Oligoasthenoteratozoospermia and infertility in mice deficient for miR-34b/c and miR-449 loci. *PLoS Genet* 10:e1004597.
37. Yuan S, et al. (2015) mir-34b/c and mir-449a/b/c are required for spermatogenesis, but not for the first cleavage division in mice. *Biol Open* 4:212–223.